

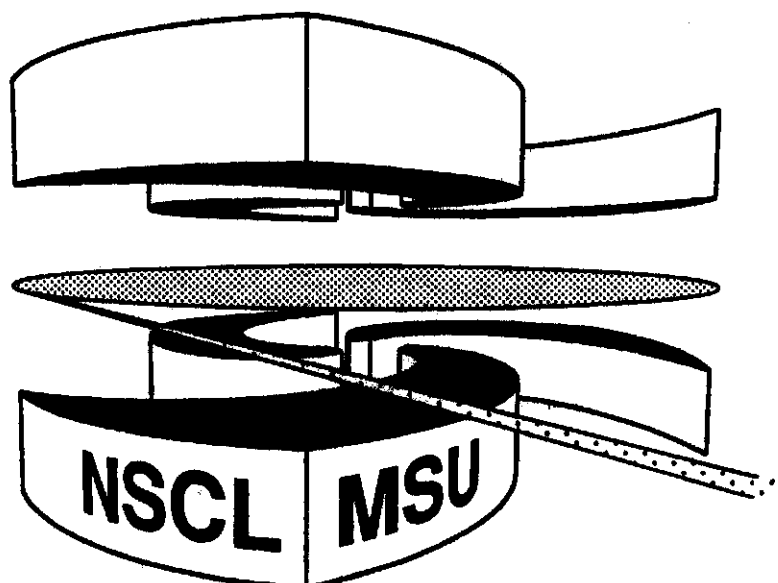


Michigan State University

National Superconducting Cyclotron Laboratory

**STUDY OF THE BREAKUP REACTION  ${}^8\text{B} \rightarrow {}^7\text{Be} + \text{p}$ :  
ABSORPTION EFFECTS AND E2 STRENGTH**

**J.H. KELLY, SAM M. AUSTIN, A. AZHARI, D. BAZIN,  
J.A. BROWN, H. ESBENSEN, M. FAUERBACH,  
M. HELLSTRÖM, S.E. HIRZEBRUCH, R.A. KRYGER,  
D.J. MORRISSEY, R. PFAFF, C.F. POWELL,  
E. RAMAKRISHNAN, B.M. SHERRILL, M. STEINER,  
T. SUOMIJÄRVI, and M. THOENNESSEN**



# Study of the Breakup Reaction ${}^8\text{B} \rightarrow {}^7\text{Be} + \text{p}$ : Absorption Effects and E2 Strength

J. H. Kelley<sup>1,2,\*</sup>, Sam M. Austin<sup>1,2</sup>, A. Azhari<sup>1,2</sup>, D. Bazin<sup>1</sup>, J. A. Brown<sup>\*</sup>, H. Esbensen<sup>4</sup> M. Fauerbach<sup>1,2</sup>, M. Hellström<sup>1,†</sup>, S. E. Hirzebruch<sup>1,\*</sup>, R. A. Kryger<sup>1</sup>, D. J. Morrissey<sup>1,3</sup>, R. Pfaff<sup>1,2</sup>, C. F. Powell<sup>1,3</sup>, E. Ramakrishnan<sup>1,2,‡</sup>, B. M. Sherrill<sup>1,2</sup>, M. Steiner<sup>1,2</sup>, T. Suomijärvi<sup>1,§</sup> and M. Thoennessen<sup>1,2</sup>.

<sup>1</sup> *National Superconducting Cyclotron Laboratory, Michigan State University, East Lansing, MI 48824*

<sup>2</sup> *Department of Physics and Astronomy, Michigan State University, East Lansing, MI 48824*

<sup>3</sup> *Department of Chemistry, Michigan State University, East Lansing, MI 48824*

<sup>4</sup> *Physics Division, Argonne National Laboratory, Argonne, Illinois 60439*

Abstract

**Distributions** of parallel and **transverse** momenta for  ${}^7\text{Be}$  fragments formed in the breakup of  ${}^8\text{B}$  have been **measured** at 41A MeV. The  $p_{\parallel}$  **distributions** are narrow ( $81 \pm 4$  and  $62 \pm 3$  MeV/c FWHM for Be and Au targets, respectively), comparable to those of neutron halo nuclei. **Reaction mechanisms influence** the  ${}^7\text{Be}$  **momentum** distributions, so they do not directly **reflect** the valence proton momentum **wavefunction**. We **present** reaction **models** that reproduce the **distributions**.

**PACS numbers:** 21.10.Ft, 25.70.De, 25.70.Mn, 27.20.+n

The proton dripline nucleus  ${}^8\text{B}$  has been the subject of considerable experimental and theoretical attention. Much of this interest concerns the possible existence of a proton halo, analogous to the extended neutron distributions that have been found around lightly bound neutron dripline nuclei such as  ${}^{11}\text{Be}$  and  ${}^{11}\text{Li}$  [1-3]. It seems that  ${}^8\text{B}$  is the most likely candidate for such a proton halo [4,5], as it is bound very weakly, by only 138 keV. Nevertheless, formation of an extended distribution by tunneling into the classically forbidden region will be hindered by the Coulomb barrier and by the angular momentum barrier seen by the  $p_{3/2}$  valence proton. It is difficult to predict whether the spatial distribution of the valence proton in  ${}^8\text{B}$  is sufficiently extended so that it forms a halo with properties essentially independent of the core, as is the case for  ${}^{11}\text{Be}$  and  ${}^{11}\text{Li}$ .

Evidence concerning the existence of a halo in  ${}^8\text{B}$  is far from convincing. Interaction cross sections measured at 790A MeV indicate a root-mean-square radius for  ${}^8\text{B}$  that differs little from those of the more tightly bound B isotopes [1,2]. However, the total reaction cross section for  ${}^8\text{B}$  appears to be enhanced in the 20-60A MeV range [6]. While the large quadrupole moment of  ${}^8\text{B}$ , compared to  ${}^8\text{Li}$ , may be evidence for a proton halo [7], E2 polarization of the  ${}^7\text{Be}$  core could also enhance the quadrupole moment [8]. Quasielastic scattering data for 40A MeV  ${}^8\text{B}$  on  ${}^{12}\text{C}$  appear to reflect the loosely bound valence proton [9], in a manner similar to that observed for the neutron halo nucleus  ${}^{11}\text{Li}$ , but the 1-proton removal cross section derived from the data of Ref. [9] does not reflect a substantial halo. Finally, and most pertinent to the subject of this letter, measurements of  ${}^7\text{Be}$  momenta resulting from the breakup of 1470A MeV  ${}^8\text{B}$  on a  ${}^{12}\text{C}$  target have been interpreted in terms of a greatly extended proton distribution for  ${}^8\text{B}$  [10].

A second reason for interest in  ${}^8\text{B}$  is that, following formation via the  ${}^7\text{Be}(p,\gamma){}^8\text{B}$  reaction, its decay produces the high energy neutrinos that dominate the response of the  ${}^{37}\text{Cl}$ , Kamiokande, and SNO neutrino detectors. The rate of the capture reaction, as summarized in the S-factor  $S_{17} = 22.4 \pm 2.1$  eV-b [11], is crucial for an understanding of neutrino production in the sun and for a resolution of the solar neutrino problem. Unfortunately, the direct measurements of  ${}^7\text{Be}(p,\gamma){}^8\text{B}$  are inconsistent. Furthermore, a recent measurement

of the cross section for the breakup reaction  ${}^8\text{B} + \gamma \rightarrow {}^7\text{Be} + \text{p}$  yielded a significantly lower value,  $S_{17} = 16.7 \pm 3.2$  eV-b [12]. However, these results are controversial because both electric dipole and electric quadrupole (E1 and E2) photons contribute to the breakup reaction [13,14]; the E2 contribution is expected to be larger than in the capture reaction because of the relatively large flux of E2 virtual photons. Theoretical estimates of the E2 contribution in the Coulomb dissociation of  ${}^8\text{B}$  are uncertain [15]. The angular distributions measured in the breakup experiment are apparently consistent with E2 contributions of zero [15]. However, this result may have a significant uncertainty because of a failure, for the high Z target, of the perturbation theory used to interpret the data.

In this letter we address these issues through measurements of the momentum spectra of  ${}^7\text{Be}$  ions resulting from the breakup of 41A MeV  ${}^8\text{B}$  ions on targets of Be and Au. Earlier we showed that core fragment momenta in the beam direction ( $p_{||}$ ) reflect the momenta of the halo neutrons in  ${}^{11}\text{Li}$  [16,17] and  ${}^{11}\text{Be}$  [18]. Thus, we expected that the widths of the observed distributions would provide a measure of the momenta of the lightly bound proton in  ${}^8\text{B}$  and then, by the uncertainty principle, the extent of its spatial distribution. Indeed we find that the distributions are much narrower than expected for fragmentation of normal nuclei; naively interpreted, these widths would correspond to an extended spatial distribution for the valence proton in  ${}^8\text{B}$ .

However, the distributions are also much narrower than the 160 MeV/c FWHM expected for a proton in a  $1p_{3/2}$  orbital [10,19]. This, coupled with the observed variation of the width with target, led us to conclude that the observed  ${}^7\text{Be}$  momentum distributions might not reflect the momentum wave function of the valence proton. In order to understand the observed widths, we investigated different reaction models for the breakup processes. For the Be target we employ a stripping model [20], and for the Au target we calculate Coulomb breakup using both perturbation theory and a dynamical model [21,22]. All of our predictions are based on the same single-particle Hamiltonian model [20], which in essence is the binding by 138 keV of a valence  $p_{3/2}$  proton in a Woods-Saxon potential ( $a=0.52$  fm,  $R=2.48$  fm); this yields a valence proton root-mean-square radius of 4.24 fm. For both

nuclear dominated breakup ( $^9\text{Be}$  target) and Coulomb dominated breakup (Au Target) the predicted fragment momentum distributions are narrower by nearly a factor of two than the valence proton momenta in the input structure model.

In the present experiment, a 200 particle-nA beam of 60A MeV  $^{16}\text{O}$  ions from the K1200 cyclotron was fragmented in a thick Be production target. Products passed through the A1200 fragment separator [23], with an Al energy absorber (wedge) placed at the second dispersive image. The beam momentum spread was limited to 0.5% by an aperture located at the first dispersive image of the A1200. The resulting beam consisted of the N=3 isotones, with a large 34.3A MeV  $^7\text{Be}$  component ( $^8\text{B}:\text{}^7\text{Be}=1:20$ ). The isotones were separated in the RPMS Wien-filter, leaving a 95% pure 41.2A MeV beam of 300  $^8\text{B}$  particles per second at the breakup target. Contaminant isotones were not completely removed by the Wien filter, because the separation slits were not positioned at the focal point. The incoming particles were unambiguously identified by their measured time-of-flight over a 40 meter flight path between a thin plastic scintillator and the detector telescopes. This insured that the detected  $^7\text{Be}$  particles came from reactions of  $^8\text{B}$  in the target.

A pair of two-dimensional position sensitive Parallel Plate Avalanche Counters (PPACs) placed upstream of the target permitted the reconstruction of the incoming particle trajectories. Breakup products were detected in two 5 cm by 5 cm  $\Delta E$ - $\Delta E$ -E telescopes. The first  $\Delta E$  detector was a position sensitive Si detector that was segmented into 16 vertical strips and 16 horizontal strips; the second was a Si PIN-diode. The E signal was provided by a stopping CsI detector. The "zero degree" telescope was 60 cm from the target and covered angles  $\theta=3.3^\circ$  to  $-1.4^\circ$  (horizontal) and  $\phi = \pm 2.4^\circ$  (vertical). A "large angle" telescope was placed 50 cm away from the target and covered the angles  $\theta = -2.6^\circ$  to  $-8.3^\circ$  and  $\phi = \pm 2.9^\circ$ . An energy calibration was obtained using  $^7\text{Be}$  beams, produced in the A1200, at 6 different energies. Backgrounds were found to be negligible from measurements with a blank target.

The results yield distributions of fragment momenta both parallel ( $p_{\parallel}$ ) and transverse ( $p_x$  and  $p_y$ ) to the beam direction. In this letter we concentrate on the  $p_{\parallel}$  distributions measured in the "zero degree" telescope, with only brief comments about the  $p_{\parallel}$  distributions measured

in the “large angle” telescope and the  $p_{\perp}$  distributions.

The  ${}^7\text{Be}$  fragment  $p_{\parallel}$  distributions measured in the “zero degree” telescope are shown in Fig. 1. The experimental effects that broaden the observed  $p_{\parallel}$  distributions are detailed, and subtracted in quadrature from the measured distributions in Table I. These include the small spread in the momentum of the incoming beam, the momentum resolution of the telescopes (0.5% FWHM after correcting for the position dependent response of the CsI detectors), and the energy spread associated with the thick Be and Au targets. The transformation into the  ${}^8\text{B}$  rest frame reduces the width by 4.4%.

In the transparent limit of the Serber model (no absorption of core fragments) [24], the  $p_{\parallel}$  distribution of heavy core fragments is identical to the projection on the beam axis of the ground state momentum distribution of the weakly bound valence nucleons. This interpretation worked well for  ${}^{10}\text{Be}$  fragments from the breakup of  ${}^{11}\text{Be}$  [18]. It was therefore surprising, at first, that the measured  ${}^7\text{Be}$   $p_{\parallel}$  distribution for the Be target is much narrower than expected for the loosely bound proton: 81 MeV/c rather than 160 MeV/c.

In the following, it will become clear that non-zero absorption of the  ${}^7\text{Be}$  core lies behind the failure of the transparent limit of the Serber model for  ${}^8\text{B}$ . It is also important that the valence proton is bound in a  $p$ -orbital. Absorption effects are much less important for weakly bound  $s$ -orbitals [20]: as noted above the transparent limit gives a good description for the  ${}^{10}\text{Be}$   $p_{\parallel}$  distributions in the breakup of  ${}^{11}\text{Be}$  where the valence neutron is in a  $2s_{1/2}$  orbital. One can obtain a rough estimate of these effects for  ${}^8\text{B}$  in a simple model. Choosing the  $z$ -axis along the beam direction, the dominant contribution to the production of  ${}^7\text{Be}$  fragments comes from  $m_{\ell} = \pm 1$  substates, because the valence proton has a much larger spatial extent in the transverse direction than in the  $m_{\ell} = 0$  substate. This allows the target nucleus to strip away the proton without disturbing the  ${}^7\text{Be}$  core. The  $p_{\parallel}$  distribution of the  $m_{\ell} = \pm 1$  substates of  ${}^8\text{B}$  has a width of about 100 MeV/c, much closer to the experimental result.

A more detailed treatment of the reaction effects was carried out [20] following the general procedures for stripping of Ref. [25]. The  $p_{\parallel}$  distribution for stripping on a Be

target, using the previously mentioned  $p_{3/2}$  ground state wave function, has a width of 82 MeV/c, in agreement with our results, as shown in Fig. 1. We have not calculated the distribution from the diffraction breakup process, that is significantly more difficult, but this distribution probably has a similar width [25,26]. We conclude from the above discussion that for light targets absorption effects greatly reduce the width of the observed  ${}^7\text{Be}$   $p_{\parallel}$  distribution compared to that of the valence proton distribution. It therefore seems unnecessary to invoke an extremely extended spatial distribution, as in Ref. [10], when the anticipated effects of absorption are included in the reaction model.

Coulomb induced breakup is expected to dominate  ${}^8\text{B}$  reactions in the Au target that yield  ${}^7\text{Be}$  in the final state. We have calculated the  $p_{\parallel}$  distribution for Coulomb dissociation on the gold target using the model of Ref. [21]. Formation of  ${}^7\text{Be}$  in its first excited state at 431 keV has been neglected; we calculate that about 3% of  ${}^8\text{B}$  breakups will form  ${}^7\text{Be}^*$ . The predicted distribution has a width of 55 MeV/c FWHM in the  ${}^8\text{B}$  rest frame and is shown by the dashed curve in Fig. 2 ( $\chi^2$  is minimized with the central 10 points for Au target predictions). Since Coulomb deflection primarily determines the  ${}^7\text{Be}$  deflection angle, we used a minimum impact parameter  $b_{\min}=40$  fm in our calculation; this value approximately corresponds to Coulomb deflection within the acceptance of the “zero degree” telescope. A calculation made with  $b_{\min}=20$  fm yields a width of 61 MeV/c, indicating an insensitivity to the precise value of  $b_{\min}$ .

The large predicted asymmetry in the Coulomb breakup distribution arises from interference between E1 and E2 amplitudes. With  $b_{\min}=40$  fm, the E2 strength contributes 9.9% of the total breakup cross section in our reaction model. The data indicate a similar but somewhat smaller asymmetry. Inclusion of higher-order dynamical processes in the Coulomb field from the gold target [22] reduces the asymmetry, as is shown by the solid curve in Fig. 2.

At large deflection angles acceptance effects [27] and reaction mechanism effects lead to broader  $p_{\parallel}$  distributions. For example, in the “large angle” telescope the corrected  $p_{\parallel}$  distribution width from breakup in the Au target is  $75\pm 6$  MeV/c FWHM (in the  ${}^8\text{B}$  rest frame); this shows the slight impact parameter dependence suggested above in the Coulomb

dissociation calculations. The broadening is much greater for breakup in the Be target ( $133\pm 19$  MeV/c FWHM, in the  ${}^8\text{B}$  rest frame); unfortunately, for nuclear dominated breakup the theory is not sufficiently developed to explain this observation.

We also obtained fragment  $p_x$  distributions by projecting  $p_\perp$  onto the horizontal x-axis. Coulomb deflection plays a leading role in determining the transverse scattering for the Au target, leading to broad distributions ( $234\pm 20$  FWHM for the Au target). For the Be target, where Coulomb effects are small, the  $p_x$  distribution width is  $87\pm 8$  MeV/c FWHM, after subtracting in quadrature the angular spread of the incoming  ${}^8\text{B}$  beam and the contribution due to multiple scattering from the measured width of  $91\pm 8$  MeV/c (Fig. 3). The gap in the distribution is due to the missing angular coverage between the two detector telescopes.

In summary, we have measured momentum distributions of  ${}^7\text{Be}$  resulting from the breakup of 41A MeV  ${}^8\text{B}$  on both light and heavy targets. The  $p_{||}$  distributions are narrower by roughly a factor of two than the distributions expected for a  $p_{3/2}$  orbital proton. Detailed models of the breakup processes are successful in explaining the data; they show that the momentum distribution of the heavy core is substantially narrower than that of the orbital proton. Our results lead to important conclusions.

First, it is not necessary to assume an unusually extended spatial distribution to explain the narrow  $p_{||}$  distributions obtained for the Be target. Nor can the data at 1470A MeV [10] be used as evidence for an extremely extended spatial wave function until reaction mechanisms effects are considered. Our results are consistent with the valence proton rms radius (4.24 fm) obtained from a standard single particle model. This radius is relatively large when compared to the radii of normal, well bound nuclei. The momentum distributions are much narrower than expected and do reflect a loosely bound proton; however, in this case the breakup mechanisms alter the connection between halo size and momentum distribution width.

And second, the distributions obtained for breakup on the Au target appear sensitive to E2 strength; predictions indicate that interference between the E1 and E2 breakup amplitudes produce an asymmetric  $p_{||}$  distribution. A high statistics measurement should provide



an accurate estimate of the E2 contribution and put Coulomb dissociation measurements of  $S_{17}$  for the  ${}^7\text{Be}(p,\gamma)$  reaction on a much firmer basis.

Finally, the valence proton wavefunction in  ${}^8\text{B}$  does not correspond to a high probability of finding the valence nucleon outside the core, as is the case for  ${}^{11}\text{Be}$  and  ${}^{11}\text{Li}$ .

This work was supported by the National Science Foundation, under grant No. PHY-92-14992 and by the US Department of Energy, Nuclear Physics Division, under Contract No. W-31-109-ENG-38.

## REFERENCES

- \* Present address Institut de Physique Nucléaire, IN<sub>2</sub>P<sub>3</sub>-CNRS, 91406 Orsay Cedex, France.
- † Present address Gesellschaft für Schwerionenforschung, Planckstraße 1, D-64291 Darmstadt, Germany.
- ‡ Present address Cyclotron Institute, Texas A&M University, College Station, Texas 77843 USA.
- § On leave from the Institut de Physique Nucléaire, IN<sub>2</sub>P<sub>3</sub>-CNRS, 91406 Orsay Cedex, France.
- [1] I. Tanihata, *et al.*, Phys. Rev. Lett. **55**, 2676 (1985).
- [2] I. Tanihata, *et al.*, Phys. Lett. B **206**, 592 (1988).
- [3] P.G. Hansen and B. Jonson, Europhys. Lett. **4**, 409 (1987).
- [4] K. Riisager and A.S. Jensen, Phys. Lett. B **301**, 6 (1993).
- [5] K. Riisager, A.S. Jensen and P. Møller, Nucl. Phys. **A548**, 393 (1992).
- [6] R.E. Warner, *et al.*, Phys. Rev. **C52** R1166 (1995).
- [7] T. Minamisono, *et al.*, Phys. Rev. Lett. **69**, 2058 (1992).
- [8] A. Csótó, Phys. Lett. B **315**, 24 (1993).
- [9] I. Pecina, *et al.*, Phys. Rev. C **52**, 191 (1995).
- [10] W. Schwab, *et al.*, Z. Phys. A **350**, 283 (1995).
- [11] J.N. Bahcall and M. Pinsonneault, Rev. Mod. Phys. **67**, 781 (1995).
- [12] T. Motobayashi, *et al.*, Phys. Rev. Lett. **73**, 2680 (1994).
- [13] K. Langanke and T.D. Shoppa, Phys. Rev. C **52**, 1709 (1995).

- [14] R. Shyam, I.J. Thompson and A.K. Ditt-Mazumder, *Phys. Lett.* **B371**, 1 (1996).
- [15] M. Gai and C.A. Bertulani, *Phys. Rev. C.* **52**, 1706 (1995).
- [16] N.A. Orr, *et al.*, *Phys. Rev. Lett.* **69**, 2050 (1992).
- [17] N.A. Orr, *et al.*, *Phys. Rev. C* **51**, 3116 (1995).
- [18] J.H. Kelley, *et al.*, *Phys. Rev. Lett.* **74**, 30 (1995).
- [19] B.A. Brown, A. Csótó, and R. Sher, *Nucl. Phys. A.* **597**, 66 (1996).
- [20] H. Esbensen, *Phys. Rev. C* **53**, 2007 (1996).
- [21] H. Esbensen and G.F. Bertsch, *Phys. Lett.* **359B**, 13 (1995).
- [22] H. Esbensen and G.F. Bertsch, *Nucl. Phys A* **600**, 37 (1996).
- [23] B.M. Sherrill, *et al.*, *Nucl. Instrum. Meth.* **B70**, 298 (1992).
- [24] R. Serber, *Phys. Rev.* **72**, 1008 (1947).
- [25] F. Barranco, E. Vigezzi and R.A. Broglia, Univ. of Milano preprint no. NTGMI-95-2.
- [26] P.G. Hansen, *Phys. Rev. Lett.* **77**, 1016 (1996).
- [27] K. Riisager, *Proceedings of the 3<sup>rd</sup> International Conference on Radioactive Nuclear Beams*, East Lansing, Michigan, Edited by D.J. Morrissey (Editions Frontieres, Gif-sur-Yvette Cedex France, 1993), p. 281. and private communication.

## FIGURES

FIG. 1. The  $p_{||}$  distributions of  ${}^7\text{Be}$  fragments from the breakup of  ${}^8\text{B}$  on a Be target. Shown with the Be target data are predictions for the  ${}^7\text{Be}$  momentum distribution in the transparent (dashes) limit of the Serber model and from a stripping model (solid) which includes the effects of absorption. The predictions, in the  ${}^8\text{B}$  rest frame, are transformed into the laboratory frame and convoluted with the experimental effects that broaden the measured momentum distribution (detailed in table 1).

FIG. 2. The central region of the  $p_{||}$  distribution from breakup in the Au target which shows the momentum distribution from Coulomb dissociation from a perturbative model (dashes) and a higher order dynamical model (solid) are shown in comparison with the Au target data. See Fig. 1 for details on the comparison of the prediction with the data.

FIG. 3. The  $p_x$  distributions of  ${}^7\text{Be}$  fragments from the breakup of  ${}^8\text{B}$  on a Be target.

## TABLES

**TABLE I. Summary of the results of the  $p_{||}$  distributions measured in the zero degree telescope.**

Target	Uncorrected	Detector resolution and	Differential E-loss	Corrected <sup>a</sup>	<sup>8</sup> B rest frame <sup>b</sup>
	FWHM ( MeV/c )	beam momentum spread, FWHM ( MeV/c )	<sup>7</sup> Be and <sup>8</sup> B ( MeV/c )	FWHM ( MeV/c )	FWHM ( MeV/c )
Be (47 mg/cm <sup>2</sup> )	86±4	13.5±1	8	85±4	81±4
Au (97 mg/cm <sup>2</sup> )	67±3	13.5±1	8	65±3	62±3

<sup>a</sup>Correction made by subtracting in quadrature columns 3 and 4 from column 2.

<sup>b</sup>Results of column 5 expressed in the rest frame of <sup>8</sup>B.

